Preparation of sustainable non-combustion filler substrate from waterworks sludge/aluminum slag/gypsum/silica/maifan stone for phosphorus immobilization in constructed wetlands

Guanghui Wang, Jingqing Gao, Rongxue Yang, Jingshen Zhang, Han Guo and Jianlei Gao

ABSTRACT

In this study, an artificial wetland filler matrix capable of effectively fixing phosphorus was prepared using a non-combustion process to save energy. To evaluate the adsorption performance of this filler, adsorption experiments were performed and the phosphorus adsorption mechanism characterization was studied. An alkaline environment was found to be conducive to the increase of adsorption capacity, but excessive alkalinity was not conducive to adsorption. Static adsorption experiments showed that the phosphorus removal rate could reach 95% in the simulated phosphorus-containing wastewater after adsorption completion. The adsorption process is closely simulated by the pseudo-second-kinetic adsorption model. The isothermal adsorption experiment data were consistent with the Langmuir and the Freundlich adsorption isotherms. The characterization results showed a large number of micropores and adsorption binding sites inside and on the surface of the filler. Speciation analysis on the adsorbed phosphorus revealed that chemisorption by calcium in this filler was the dominant adsorption mechanism. The research results of this study provide the basis and reference for the development of high-efficiency phosphorus removal filler in constructed wetlands.

Key words | adsorption mechanism, efficient phosphorus removal, non-combustion filler, transformation and migration of phosphorus

Guanghui Wang
Jingqing Gao (corresponding author)
Rongxue Yang
Jingshen Zhang
Han Guo
Jianlei Gao
School of Water Conservancy and Environment,
Zhengzhou University,
Zhengzhou 450001, Henan Province,
China
E-mail: *jingqinggao@zzu.edu.cn*

Jingqing Gao
Jingshen Zhang
Zhengzhou Yuanzhihe Environmental Protection Technology Co., Ltd,
Zhengzhou 450000, Henan Province,
China

INTRODUCTION

The problem of phosphorus-rich water caused by the extensive use of fertilizers increases their presence in wastewater and is becoming an important issue in urban development (Wei *et al.* 2008; Tercero *et al.* 2017). In recent years, constructed wetland filler materials rich in aluminium, calcium, iron and magnesium have been favoured by researchers. These materials tend to have strong active adsorption characteristics and low cost. In the production process, many researchers used high temperature for firing. As an industrial production waste, lime slag is directly mixed with fly ash and different additives (shale, perlite, diatomaceous earth and sawdust) to prepare ceramsite by a granulation and sintering process (Qin *et al.* 2015). Some sintered clay materials expand inside the system under high temperature conditions (Xu *et al.* 2009). In the past, such fired fillers have found wide application in constructed wetlands, but they have disadvantages, including high energy consumption, high cost, high pollution, low recoverability and more.

In contrast, the non-combustion method saves energy and is environmentally friendly, and the cost is low. Non-combustion filler in China is still in a developing stage, and the product has problems such as high bulk density, low strength and small specific surface area. Non-combustion fillers have good application prospects, and some scholars have conducted research in this area.

Gypsum is a very common material and is widely used in adsorbent materials. We analysed a gypsum material and found that it is mainly a calcium compound. Using a filler made of gypsum, it was found that the hardening

doi: 10.2166/wst.2019.258

speed was fast and the hardness was high. The benefit of gypsum lies in its role as a skeleton builder to help or enhance the interaction between polymer and sludge particles and to build up a more rigid lattice structure (Zhao 2006). Batch studies indicated that more than 95% of P can be rapidly (<1 h) removed by thermally treated calcium-rich attapulgite (TCAP) from solution with a concentration of 20 mg P/L (Yin *et al.* 2017). Silica and gypsum have similar crystal structures, so silica is added as a hardening material. An artificial wetland filler made of gypsum and silica has not been found domestically or internationally; its invention is the biggest innovation of this study. Scholars have studied the adsorption of phosphorus by using waterworks sludge, which is a good resource that can be reused. The research on the utilization of waterworks sludge is of great significance. Babatunde & Zhao (2010) further demonstrate that alum sludge, a widely available by-product of water treatment plants, can be used as a cost-effective adsorbent for P in aqueous solutions. Phosphorus removal at the laboratory scale was studied on unvegetated vertical subsurface flow constructed wetland systems using alum sludge as the main substrate (Babatunde & Zhao 2009). As a main by-product of the aluminium industry, aluminium slag has shown good capability for removing phosphate from water. Maifan stone is often used in water treatment, and its main component ratio is: Si: O: C: Al: Na: K: Ca = 60.14%: 18.23%: 8.55%: 1.50%: 0.64%: 0.41%: 0.37%. The increase in the surface roughness with the maifan stone improves the contact between sewage and the adsorbate to achieve the purpose of phosphorus removal.

In this study, a new type of waterworks sludge-based non-combustion filler was first prepared by using gypsum, silica, waterworks sludge and aluminium slag, and then the maifan stone was added to the filler. The proportion of the addition was based on the single factor design test result. The raw materials for the adsorption material was finally selected after a large number of repeated experiments. This research is to innovate a new type of waterworks sludge-based non-combustion filler and improve the pollutant phosphate removal ability of the filler matrix.

MATERIALS AND METHODS

Filler preparation

The water content of the waterworks sludge obtained from the waterworks was above 95%. A filter press was used for dewatering. The sludge was left in the air and continued to dry naturally. After drying in a constant temperature drying (105 °C) oven, the sludge was pulverized using a mortar. The waterworks sludge was passed through a sieve with a 200 mesh size. After sieving, it was placed in a desiccator and stored for later use. The waterworks sludge and aluminium slag were subjected to thermal modification pretreatment at 105 °C, and dried for 2 h. According to the ratio (the ratio of waterworks sludge, aluminium slag, gypsum, silica and maifan is 4:4:10:1:1), they were evenly mixed. Due to the iron, calcium, and aluminium, the filler had good phosphorus adsorption properties. A NaOH solution (1 mol/L) was continuously added, and the mixture was uniformly stirred to obtain a spherical granularity. The physical indices of the filler (density level, performance density, bulk density, water absorption and voidage) were determined after granulation.

Serial adsorption experiments

All static adsorption experiments were performed in 250 mL volume conical flasks. A solution of KH_2PO_4 was used as the simulated wastewater in this experiment, and the volume of solution added was 50 mL. Since the filler is rich in phosphorus-absorbing components, it was expected that the filler would effectively remove KH_2PO_4. For kinetic studies, 1 g of the filler was ground into powder and placed in the simulated wastewater, the pH of the solution was adjusted by using HCl and NaOH, and the filler was shaken for 30 h in a constant-temperature oscillator. The content of phosphorus in the solution was measured at different times. The initial concentration of P ranged from 5 mg/L to 20 mg/L.

For the adsorption isotherm experiment, the amount of filler added was 20 g/L, and the mixture was shaken at different temperatures for 24 h in a constant-temperature oscillator. Simulated wastewater with different concentration gradients was placed in 250 mL conical flasks, and the adsorption and equilibrium concentrations were determined.

To investigate the effect of the filler addition amount on the adsorption of phosphorus, different quality fillers (filler dose: 10 g/L, 15 g/L, 20 g/L, 25 g/L, 30 g/L) were added to the simulated wastewater, and the mixture (pH = 7) was shaken in a constant-temperature oscillator for 24 h. The initial pH of the solution was adjusted to 7 with 0.5 mol/L HCL or NaOH. The adsorption process was carried out in a temperature-controlled shaker (25 °C, 160 rpm). After certain treatment of the oscillating fluid, the adsorption capacity was calculated.

Studies have shown that the phosphorus adsorption process by the filler is closely related the pH of the liquid. Different pH environments affect the final adsorption. To study this, the following experiment was performed: 50 ml wastewater was put into six equal-sized conical flasks, and the pH of the liquid in the six bottles was adjusted to 6, 7, 8, 9, and 10, respectively. The filler addition amount was 20 g/L, and the P content was 20 mg/L. After the adsorption was completed, the adsorption amount and the removal rate were evaluated.

The calculation formulas for the adsorption amount and the removal rate are as follows.

$$Q_e = \frac{(C_0 - C_e)V}{m} \quad R\% = \frac{C_0 - C_e}{C_0} \times 100\% \tag{1}$$

Q_e represents the equilibrium adsorption amount, C_0 represents the initial phosphorus concentration, C_e represents the concentration of phosphorus at equilibrium, V represents the volume of the simulated wastewater, and m represents the amount of filler added. R% represents the phosphorus removal rate.

Analytical methods and quality control

The waterworks sludge was sourced from the Wulongkou Waterworks (Zhengzhou, Henan China), and the gypsum, silica and maifan stone were sourced from the high-tech zone construction market (Zhengzhou, Henan China).

The solution pH was monitored with a standard pH meter (Shanghai Sheng Ci PHS-3C precision pH meter digital display desktop acidity meter). Three parallel experiments were undertaken in each experimental group and the experimental results, including error bars, were calculated. The orthophosphate was measured using the Chinese standard method. The instrument used was the intelligent multi-parameter water quality analyser of China Lianhua Technology Co., Ltd. The model of the instrument was 5B-3B (V8), and the total phosphorus range was 0.01 mg/L–0.6 mg/L. The reagent used in the measurement process was a special measurement consumable provided by this company. The solid in the water sample was centrifuged at 4,000 rpm for five minutes before the measurement, and the supernatant was filtered through a 0.45 mm membrane filter. The final adsorption liquid was the liquid filtered by the filter membrane. The oscillator was the STIK® company's INCUBATOR SHAKER SERIES PSE-T150. For quality assurance and control, the blank sample and the standard water sample were treated in the same way to evaluate the phosphorus content of the water sample and the phosphorus adsorption effect of the filler.

Material characterization

The filler performance indicators include density level, performance density, bulk density, water adsorption and voidage. The specific experimental methods were as follows. Density level: The filler pressurization force was measured by a press, and the density rating was determined according to the Chinese light aggregate standard. Performance density: An electronic analytical balance was used to measure the dry weight, and the samples were placed vertically in the measuring cylinder. The volume value of the corresponding measuring cylinder was read, corresponding to the upper surface of the upper filler. The mass-to-volume ratio is the performance density. Bulk density: The filler was placed in water for approximately 1 h until it reached water absorption saturation, and then it was placed in a measuring cylinder filled with an appropriate amount of water. The difference between the volume values of the scale lines corresponding to the water surface is the volume of the filler. The mass-to-volume ratio is the bulk density. Water absorption: The filler was placed in water for approximately 1 h until it reached water absorption saturation. The ratio of the difference in mass before and after water absorption to the dry mass is the water absorption rate. Voidage: The ratio of the difference between performance density and bulk density to the performance density is the voidage.

X-ray diffraction (XRD) can be used to perform phase analysis. The instrument used for XRD analysis was the X'pert PRO of Netherlands PANalytical. A surface morphology analysis was carried out by using scanning electron microscopy (SEM), using a British Carl Zeiss Sigma 500. To investigate the composition properties and apparent changes of the filler before and after adsorption, comparative analysis was made in two states. SEM and XRD analysis were performed at the Experimental and Analytical Testing Center of the School of Chemistry and Molecular Engineering, Zhengzhou University, China's State Key Laboratory.

RESULTS AND DISCUSSION

Analysis of filler properties

After the preparation of the filler in this experiment, it was placed in room temperature conditions for 2 h, and then

Table 1 | Filler property parameters

Filler parameter	Numerical value
Density level	400
Bulk density	816.96 kg/m^3
Performance density	1436.1 kg/m^3
Water absorption	24.64%
Voidage	42.89%

transferred into a constant-temperature drying oven and dried at 105 °C for 2 h. After that, the filler was placed in a ventilated place in a natural environment and dried naturally. As a kind of wetland filler, it was essentially an artificial light aggregate. According to China's requirements for artificial light aggregates, the filler produced in this study belonged to the light and coarse aggregate, and the specific filler property parameters are shown in Table 1. Additionally, other properties (grain size, grain size distribution and Mohs hardness) were measured. The grain size and grain size distribution results are shown in Figure 1. The grain size is 342 nm and the Mohs hardness is 2.

There were three stages in the process of curing the filler: hardening, drying, and natural curing. During the hardening process, part of the surface of the filler began to evaporate, and various substances in the filler condensed and hydrated to form a mixed cementitious material. This was an early curing process, which was mainly material hardening. At this stage, the filler already had a preliminary strength, which prevented the surface of the filler from cracking due to an increase in temperature during the drying process. The drying process was mainly carried out in a constant-temperature drying oven. In the drying stage, the free moisture in the filler gradually decreased with increasing temperature and drying time, so that the parts of the filler would become closer together with less space between the particles. Additionally, the filler strength was further enhanced. Drying under natural conditions was the last stage, and the dehydration of the filler raw materials led to a further increase in the filler hardness. The compressive strength (pressure under crushing) was measured every day during the filler curing process. As time passed, more and more hydration products were formed, and the strength increased more rapidly. After a certain period of time, the strength growth gradually slowed.

The surface of the filler was light yellow, because of the addition of a large amount of waterworks sludge and aluminium slag powder. In the early stage of drying, due to the addition of gypsum, the rate of hardening and coagulation was fast, and a white colour on the surface of the filler was typical. In the later stage of granulation, this phenomenon gradually disappeared. The stability characteristic was measured. The filler was soaked in water and surface changes were observed regularly. A large amount of water was absorbed in the beginning due to the small gaps inside the filler. After soaking for about one week, a slight partial dissolution of the filler surface occurred due to the addition of water. A small number of dissolved yellow particles appeared in the water. However, in general, the filler was still high in hardness and had high stability, which is very important in the practical substrate application to constructed wetland.

ANALYSIS OF ADSORPTION RESULTS

Effect of adsorbent dose

To explore the effect of adsorbent dose, related experiments were conducted to explore the results, as shown in Figure 2(a). As the dose amount increased, the equilibrium

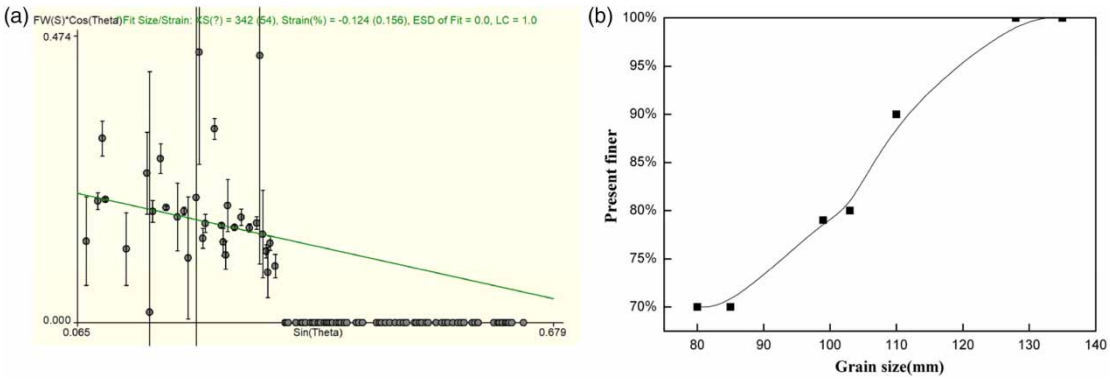

Figure 1 | Grain size (a), distribution of grain size (b).

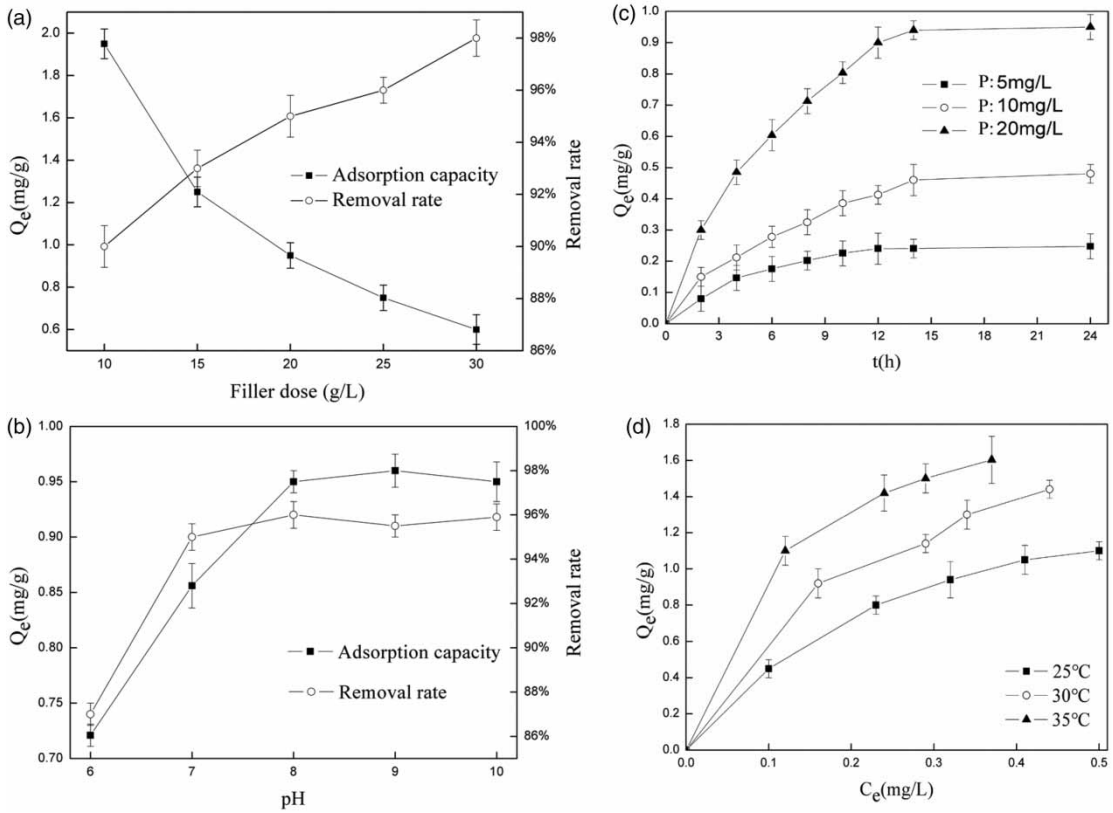

Figure 2 | Effect of filler dose (a), effect of pH (b), kinetic curves (c), isothermal adsorption curves (d). Experimental condition: volume of the solution was 50 mL, filler dose was 20 g/L.

adsorption capacity decreased. When the dose was changed from 10 g/L to 30 g/L, the amount of adsorption changed from 2 mg/g to approximately 0.6 mg/g. The removal rate varied from 90% to 98% when the dose varied, which could be seen as complete adsorption at a filler dose of 30 g/L.

This is easily understood from the viewpoint of Formula (1). As the amount of additive increased, the adsorption capacity decreased, and naturally, the phosphorus removal rate increased. When the dose was increased, the total amount of filler increased, and the resulting increase in adsorption sites in the entire solution increased the adsorption capacity. The content of residual phosphorus in the solution decreased. In other words, the adsorption amount increased and the adsorption capacity decreased. In combination with various factors, the adsorbent dose selected in this experiment was 20 g/L.

Effect of initial pH

The result (Figure 2(b)) shows that the phosphorus removal capacity and removal rate increased with increasing pH value within a certain range. For pH = 6–9, the adsorption amount gradually showed an increasing trend with the increase in the solution alkalinity, and showed a slow growth trend near pH = 10. For lower pH values (an acidic environment), the amount of phosphorus adsorbed was 0.7 mg/g. The adsorption capacity at this time was much lower than that under normal conditions. While the pH changed from 6 to 10, the adsorption amount changed from 0.7 mg/g to 0.95 mg/g, and the removal rate also varied between 86% and 95%.

Figure 2(b) indicates the filler exhibited good adsorptivity under neutral and alkaline conditions. A conclusion could be drawn from the slope of the line in this graph that the adsorption performance was greatly affected by the acidity, while the adsorption performance in the neutral and slightly alkaline environments tended to rise, but in the highly alkaline environment, it showed poor growth of adsorption ability. If the filler in this study was actually applied to the constructed wetland, the pH of the sewage to be treated could be adjusted to the medium alkaline range to maximize the filler adsorption performance.

Adsorption kinetics

The effect of contact time is also important, and adsorption kinetics evidently controls the process at the solid-solution interface. Figure 2(c) illustrates the effect of different contact times on phosphorus adsorption. Figure 2(c) shows that the adsorptive quantity of phosphorus increased with increasing contact time. A two-stage kinetic behaviour was evident: an initial rapid stage in which adsorption was fast and contributed significantly to equilibrium uptake, and a slower second stage, the contribution of which to the total phosphorus adsorption was relatively small. For different initial concentrations, the time to reach the adsorption equilibrium was roughly the same, starting at approximately 10 h to reach equilibrium, and reaching full adsorption saturation at approximately 14 h. After the completion of adsorption in the three experimental groups, the phosphorus removal rate exceeded 95%. Obviously, as the initial concentration of the liquid increased, the adsorption capacity at equilibrium also increased.

An analysis of the equilibrium data and kinetic data were important to develop an equation which accurately represented the results and which could be used for design purposes (Han *et al.* 2008). Adsorption kinetics models were used to explain the adsorption mechanism and adsorption characteristics. Three simple kinetic models (pseudo-first-order, pseudo-second-order (Jie Fu *et al.* 2010) and the Elovich equation) are commonly used to fit the filler phosphorus adsorption effect to explore the adsorption type.

$$Q_t = Q_e(1 - e^{-k_1 t}) \quad \text{The pseudo-first-order equation} \tag{2}$$

$$\frac{t}{Q_t} = \frac{1}{k_2 Q_e^2} + \frac{t}{Q_e} \quad \text{The pseudo-second-order equation} \tag{3}$$

$$Q_t = a + b \ln t \quad \text{The Elovich equation} \tag{4}$$

Q_e is the equilibrium adsorption amount, mg/g. Q_t is the amount of adsorption at each moment in the adsorption process, mg/g. k_1 is the adsorption rate constant of the first-order adsorption equation, h^{-1}. k_2 is the adsorption rate constant of the second-order adsorption equation, g/(mg·h). a and b are the Elovich constants.

The results of the two kinetic fitting equations are shown in Figure 3(a)–3(c). The correlation coefficient R^2 of the pseudo-first-order kinetic equation is 0.86722, the correlation coefficient R^2 of the pseudo-second-order kinetic equation is 0.94228, and the correlation coefficient R^2 of the pseudo-second-order kinetic equation was 0.90543.

These three models can predict the kinetic processes in experimental conditions. Moreover, the best model was the pseudo-second-order model, while the worst model was the pseudo-first-order model. Therefore, the pseudo-second-order model can be used to predict the kinetic process of phosphorus adsorption. The pseudo-second-order model indicates that the rate-controlling step for phosphorus adsorption is a chemical interaction (Liu *et al.* 2015). When the solid is in contact with the liquid, ion exchange occurs between the two. Due to the concentration and type of the ion, chemical precipitation occurs inside the filler and on the surface, and a precipitate of the phosphorus-containing compound is formed, which settles at the bottom of the liquid.

The adsorbate transport from the solution phase to the surface of the adsorbent particles occurs in several steps. The overall adsorption process may be controlled by one or more of the following steps: film or external diffusion, pore diffusion, surface diffusion and adsorption on the pore surface. The possibility of intra-particle diffusion was explored by using the intra-particle diffusion mode.

$$Q_t = Kt^{\frac{1}{2}} + C \tag{5}$$

where K is the intra-particle diffusion rate constant, and C is the constant that indicates the thickness of the boundary layer (larger values of C indicate greater boundary layer effects).

In the fitted equation for intra-particle diffusion mode (Figure 3(d)), the first straight line describes the pore diffusion of the macroscopic filler, and the second part describes the microscopic pore diffusion. The constants of C are not zero, for the lines did not pass through the origin. This indicates that pore diffusion did not limit the adsorption rate. Therefore, the adsorption process is a complex process consisting of surface adsorption and intraparticle diffusion.

Based on the adsorption kinetics curve, the filler adsorption process can be characterized by 'rapid adsorption and slow equilibrium'. During the period of 0–10 h, the amount of phosphorus adsorbed by the filler increased rapidly with time. This was because at the initial stage of the adsorption process, there were more active adsorption sites on the filler surface, which adsorbed many ions. The concentration gradient of adsorbed substances formed on the solid–liquid surface was also large, which was beneficial to physical adsorption and ligand exchange with the adsorption sites in the filler surface (Yang *et al.* 2006). This period of time was a rapid adsorption process, but as the adsorption

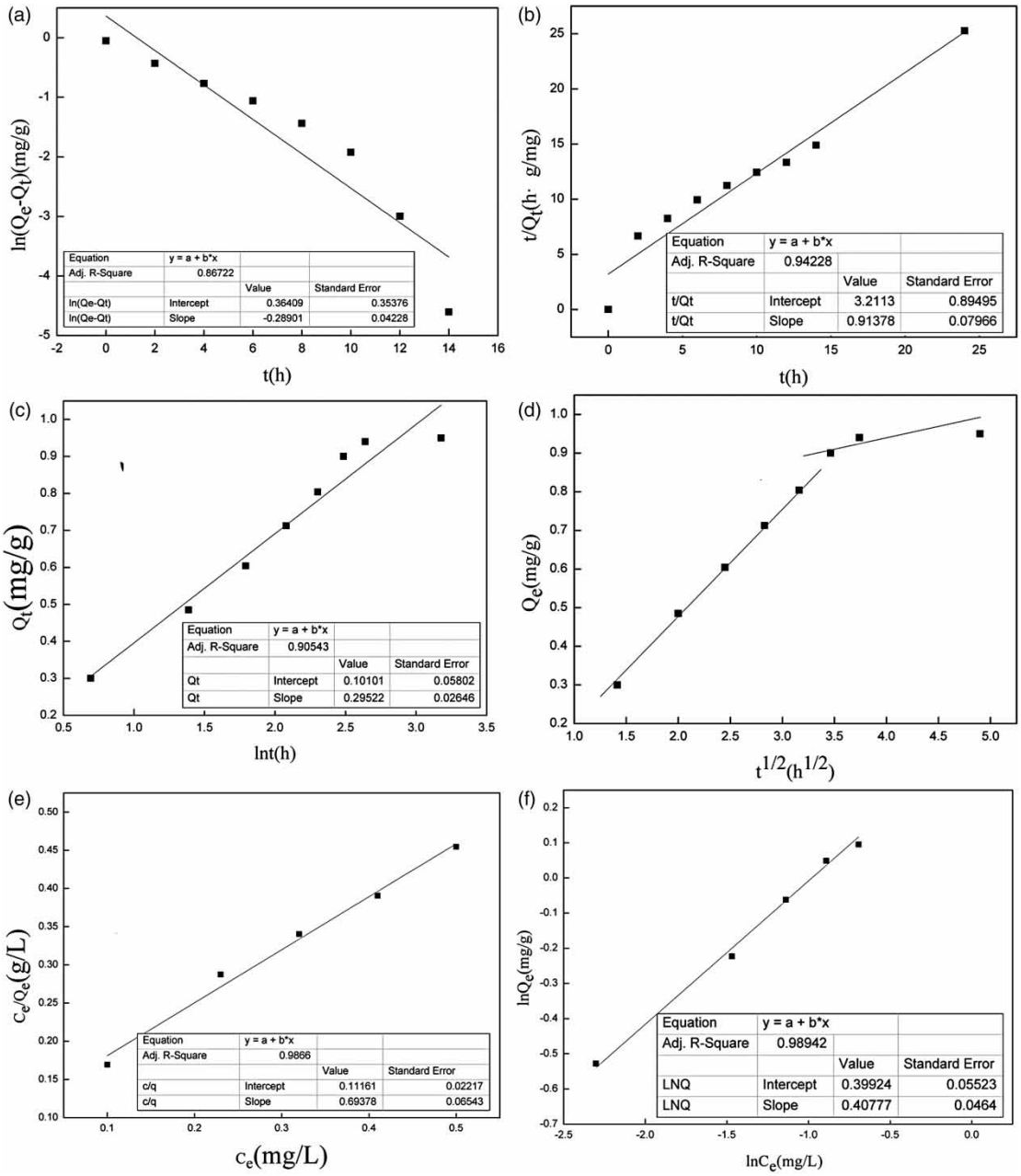

Figure 3 | Adsorption model simulation results. Pseudo-first-order equation (a). Pseudo-second-order equation (b). Elovich equation (c). Intra-particle diffusion mode (d). Langmuir adsorption model (e). Freundlich adsorption model (f).

time was prolonged, the active adsorption sites on the filler surface gradually decreased, and the rate of the adsorption reaction slowed. In this process, the phosphorus was adsorbed by the diffusion of the internal microporous mesoporous of the filler (Babatunde *et al.* 2009). This was a slow adsorption process. With increasing initial phosphorus content, the phosphorus adsorption amount was significantly increased, because the exchange driving force generated under the condition of high phosphorus concentration was large, so the adsorption sites on the filler surface could adsorb enough phosphorus.

Adsorption isotherm

From the isothermal adsorption diagram (Figure 2(d)), the increase in the equilibrium concentration led to the increase of adsorption capacity. The filler adsorption process showed a tendency to rapidly increase the adsorption amount at

first, and then slow with increasing equilibrium concentration. Additionally, the adsorption capacity increased as the temperature increased from 25°C to 35°C, indicating that temperature affects the adsorption process. The filler equilibrium adsorption capacity at the same concentration increased with increasing temperature.

To further explore the adsorption type, it is necessary to study the adsorption type and adsorption model. The isothermal adsorption model was established based on the experimental data, and two representative models – the Langmuir and Freundlich models (Jie Fu & Zhua 2010) describe it.

The Langmuir adsorption isotherm

$$\frac{C_e}{Q_e} = \frac{1}{K_L Q_m} + \frac{C_e}{Q_m} \tag{6}$$

The Freundlich adsorption isotherm

$$\ln Q_e = \ln K_F + \frac{\ln C_e}{n} \tag{7}$$

Q_e is the adsorption capacity of phosphorus at equilibrium, mg/g. C_e is the concentration of phosphorus at equilibrium, mg/L. K_L is the Langmuir constant related to the adsorption energy, L/mg. K_F is the Freundlich constant related to adsorption capacity, L/mg. n is the heterogeneity factor, indicating the adsorption intensity of the adsorbate.

This study used 30 °C as an example to fit an equation to the data (Figure 3(e) and 3(f)). In general, the larger K_F is, the larger the heterogeneity, and the larger the value of 1/n is, the more spontaneous the adsorption process. The correlation coefficient R^2 of the Langmuir adsorption isotherm was 0.9866, and the correlation coefficient R^2 of the Freundlich adsorption isotherm was 0.98942, so the Langmuir adsorption isotherm and the Freundlich adsorption isotherm can both simulate the isotherm adsorption process. In the adsorption process, due to the gap between the particles, there are both reversible adsorption processes (single layer adsorption) and chemical precipitation processes (multilayer adsorption). And in the isothermal adsorption model, they all have high correlation coefficients.

The ambient temperature is a very important factor that affects the adsorption behaviour. The increase in temperature contributes to the diffusion of phosphorus compounds, which exacerbates molecular motion and accelerates the adsorption process. A violent desorption process was also taking place with the increase in temperature. The reason was that high temperature was favourable for the formation of hydrogen bonds, and the adsorption was more stable, and the electrostatic action was also easily destroyed. The higher temperature promoted the progress of the adsorption process; from a thermodynamic point of view, the reaction was endothermic, which proves the adsorption process is a chemical reaction rather than a physical adsorption.

Characterization of adsorbent and mechanism research

To understand more about the surface morphology and crystalline phases of the filler bodies, SEM analyses were conducted. The SEM images (Figure 4(a)) show that the filler had layered discontinuous segments, its surface was rough, loose and cracked, the pore distribution was relatively uniform, and the number of small grains was high. The surface had lamellar morphology and the structure was fragmented and loose. Rough surfaces are conducive to improved contact between the filler and the adsorbent, and the large number of pore channels is conducive to the ion exchange. On the surface of the filler after adsorption (Figure 4(b)), some cellular microporous structures were found, which were identified as silicon and its compounds. Their presence might be due to the inclusion of silica in the filler material or the inclusion of some clay particles in the stone. These microporous structures were not fully opened prior to adsorption. These microporous structures exerted a strong adsorption capacity when the surrounding environment contained a large amount of phosphorus and its compounds, and its unique structure also contributed to the completion of adsorption. Moreover, it was also apparent that the filler surface after adsorption had an increased number of layered structures, the original smooth surface became rough, and the unique multilayer structure contributed to the improved filler adsorption performance. The surface of the filler was characterized by a large number of particles, small pores, thin boundaries and large cracks. The change in the number of micropores after water absorption had a great influence on the structures on the filler surface. Unlike the unfired filler, the fired filler microstructure is mainly due to the melting of the raw materials, the reorganization of the components, the formation of a large number of bubbles and pores, and some complex crystals. The non-combustion filler is mainly a combination of gypsum and silica, which were condensed with each other in an alkaline environment to form a cementitious material similar to cement.

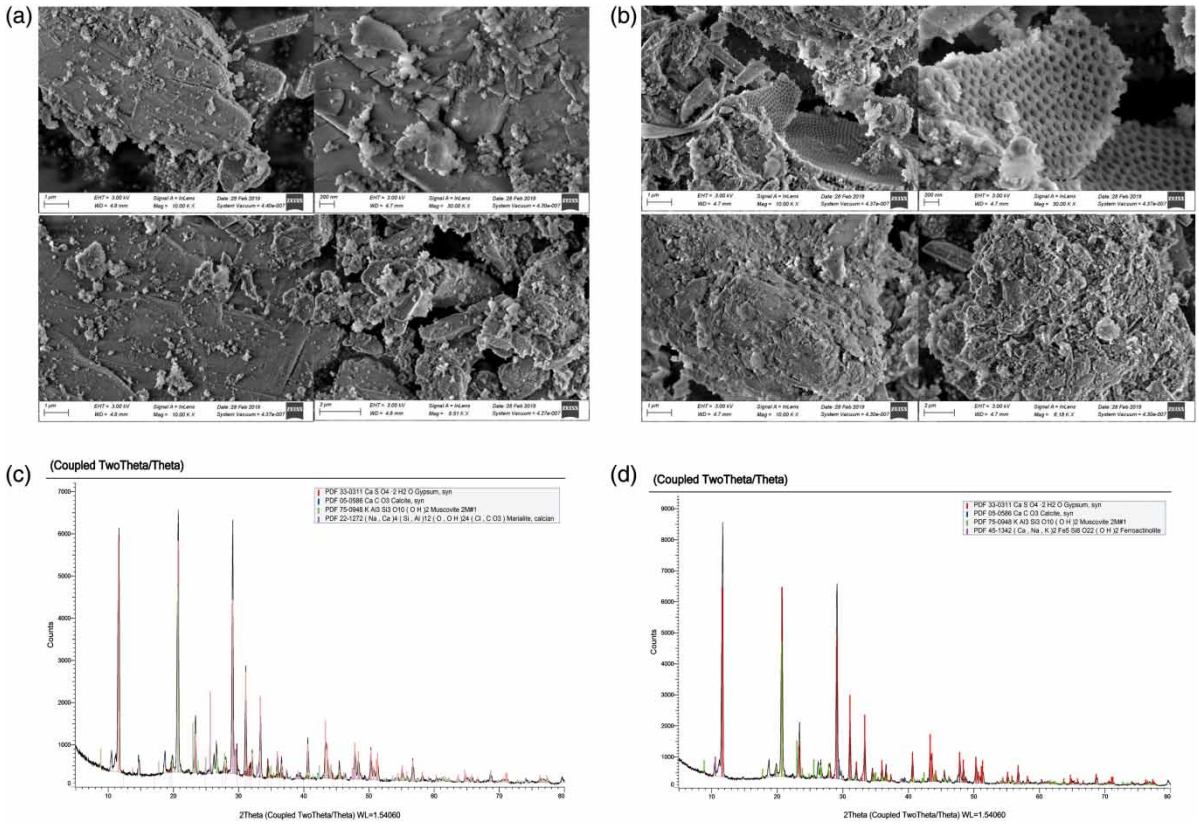

Figure 4 | Characterization results. SEM image before (a) and after (b) the adsorption. XRD image before (c) and after (d) adsorption.

In this study, XRD analyses were performed to obtain the mineral compositions of filler specimens by using an XRD pattern database (International Centre for Diffraction Data, ICDD). The filler adsorption state is readily apparent from the spacing of the test material layers. In the smaller area of 2θ, a very obvious high and narrow characteristic diffraction peak can be seen. It reflects that the grain surface growth of the filler particles is high and the crystal is good. Figure 4(c) shows that the main filler components are $CaSO_4{\cdot}2H_2O$ (gypsum), $CaCO_3$ (calcite), $KAl_3Si_3O_{10}(OH)_2$ (muscovite) and some main material of Marialite. After adsorption, the main components of Ferroactinolite were found in the filler. In the analysis of the experimental results, using the professional XRD analysis software Jade 6.5, a large amount of $CaPO_3(OH){\cdot}2H_2O$ (intensity count (IC): 97%), $(NH_4)_2HPO_4$ (IC: 54%), $Ca_4Al_2O_6CO_3{\cdot}11H_2O$ (IC: 92%) and $K_2H_2P_2O_7{\cdot}0.5H_2O$ (IC: 54%) was found in the adsorbed filler (Figure 4(d)), and there was little $Fe_5(PO_4)_4(OH)_3{\cdot}2HO$ (IC: 5%). The XRD results show that the filler has a good adsorption effect, and a large amount of phosphorus-rich precipitate was formed. In the study, in addition to phosphorus, some other components were changed due to the presence of a large amount of phosphorus in the aqueous solution. So, from the XRD diagram, the filler has a good removal effect on phosphorus due to the types of elements and compounds it contains.

The filler phosphorus adsorption process can be divided into two processes. During the first process, the phosphorus compound was gradually transferred from the liquid phase body to the filler surface. The second process was the diffusion of the phosphorus compound inside the filler. Since the initial concentration of phosphorus was high, the resistance to separation from the liquid phase water solvent to the filler surface was large, which caused the speed from the aqueous phase to the outside of the filler to be slow. However, inside the packing, the situation was reversed, and the diffusion and transfer of the phosphorus compound was easier and faster. This is because inside the packing, the phosphorus compound is surrounded by tiny pores with strong adsorption in the space. From the perspective of the overall adsorption process, when the concentration was high, the external diffusion and transfer process played an important leading role. When the concentration was low, its diffusion

inside the filler was the main factor controlling the adsorption rate.

The chemical composition, the morphological structure and the surface characteristics of the filler may affect the adsorption mechanisms and should be considered as part of the research to understand the adsorption mechanism. Adsorption is reversible. Chemisorption is the interaction of the adsorbed substance with the surface, building new substances. The XRD results show that a compound containing phosphorus was formed. There are two competing processes (phosphate adsorption and phosphate precipitation) to P-removal (Chen *et al.* 2013). The chemical precipitation rather than adsorption was proposed to be the phosphorus removal mechanism by some Ca-rich materials such as slags (Barca *et al.* 2013). The highly correlated pseudo-second-order kinetic equation also shows that the adsorption of phosphorus by the filler is chemical precipitation. The composition and structure of the filler provide good adsorption conditions, and the adsorption effects may be different for different environments. Combining the results of two adsorption models, the adsorption mechanism is chemical precipitation and ion adsorption.

For the adsorption process inside the packing, the diffusion was driven by the concentration gradient between the surface of the packing and the adsorption sites inside the particles. At higher solution loads, it had a higher surface load, so a larger concentration gradient was formed between the surface and the interior, driving a large amount of phosphate to diffuse from the surface to the deeper particles. The resulting combination is usually irreversible (Clark *et al.* 2012). An irreversible reaction process illustrates that the phosphorus adsorption by the filler is chemisorption. According to existing research, the adsorption of the filler in constructed wetland was the main removal method (Yang *et al.* 2001). The chemical adsorption of the filler is the main mechanism of action of adsorption (Vohla *et al.* 2011). From the material analysis of XRD and SEM, the filler has a good adsorption composition and structure. The chemisorption of phosphorus by fillers is related to many factors. For example, the effects of pH, calcium ions, iron ions, aluminium ions and their oxides, adsorption and precipitation by coordination compounds, generally produce poorly soluble precipitates to achieve removal. Phosphorus in sewage has different states under different pH conditions, as shown in Table 2. The specific precipitation reaction carried out under different pH conditions is shown in Table 3. The conditions under which different reactions occur are different solubility products of different precipitates, so different precipitation reactions occurred under different pH conditions.

Table 2 | Existing form of inorganic phosphate in water at different pH values

pH	Inorganic phosphate form
4.0–7.0	HPO_4^{2-}, $H_2PO_4^-/HPO_4^{2-}$ has a high concentration
7.0–10.0	HPO_4^{2-}, $H_2PO_4^-/H_2PO_4^-$ has a high concentration
10.0–12.0	HPO_4^{2-} is most, PO_4^{3-} is seldom
>12.5	HPO_4^{2-} is most

Table 3 | Precipitation reaction of phosphate at different pH values

pH	Precipitation reaction
5.0–7.0	$Fe^{3+} + H_nPO_4^{-3+n} \rightarrow FePO_4\downarrow + nH^+$, $Fe(OH)_3 + H_2PO_4^- \rightarrow FePO_4\downarrow + OH^- + 2H_2O$
6.0–8.0	$Al^{3+} + H_nPO_4^{-3+n} \rightarrow AlPO_4\downarrow + nH^+$, $Al(OH)_3 + H_2PO_4^- \rightarrow AlPO_4\downarrow + OH^- + 2H_2O$
>8.0	$Ca^{2+} + OH^- + HPO_4^{2-} \rightarrow Ca_3(PO_4)_2\downarrow + H_2O$, $5Ca^{2+} + 4OH^- + 3HPO_4^{2-} \rightarrow Ca_5(OH)(PO_4)_3\downarrow + 3H_2O$

As shown in Table 3, at pH 5–7, mainly Fe^{3+} reacts with its hydrated oxides and hydroxides and phosphate ions; at pH 6–8, it is mainly Al^{3+} and its hydrated oxides. The hydroxide participates in the reaction; when the pH is above 8, mainly the Ca^{2+} ion adsorbs phosphorus. The neutral and alkaline environment facilitates the conversion of phosphate and combines with the active calcium in the filler to form a $Ca_3(PO_4)_2$ precipitate. If the water environment is highly alkaline, then the precipitated $Ca_3(PO_4)_2$ will be further converted into $Ca_5(PO_4)_3OH$ with higher hydroxyl stability. Moreover, $Ca_5(PO_4)_3OH$ is the most thermodynamically stable and most difficult to solubilize. However, under more acidic conditions, $CaHPO_4$, $Ca_4H(PO_4)_3$, and $Ca_3(PO_4)$ are thermodynamically more stable (Chen *et al.* 2013).

CONCLUSIONS

The filler in this study is a new type of non-combustion filler made from feed waterworks sludge and aluminium slag as its main components. It has the advantages of energy savings and environmental protection, as well as a good phosphorus removal effect. The filler phosphorus adsorption capacity increases with increasing contact time, reaching equilibrium after approximately 10 h. The adsorption rate is first fast and then slower, which is consistent with a pseudo-second-order kinetic adsorption model. The

isothermal adsorption process follows the Langmuir and Freundlich isotherm models. The research results of this paper provide the basis and reference for the development of high-efficiency phosphorus removal filler in constructed wetland.

ACKNOWLEDGEMENTS

The authors gratefully acknowledge the financial support by the Key R&D and Promotion Project of Henan Province (192102310498), Major Special Science and Technology Project of Henan Province (181100310300) and National Science and Technology Major Project (2017ZX07602-003-002).

REFERENCES

Babatunde, A. O. & Zhao, Y. Q. 2009 Phosphorus removal in laboratory-scale unvegetated vertical subsurface flow constructed wetland systems using alum sludge as main substrate. *Water Science and Technology* **60** (2), 483–489.

Babatunde, A. O. & Zhao, Y. Q. 2010 Equilibrium and kinetic analysis of phosphorus adsorption from aqueous solution using waste alum sludge. *Journal of Hazardous Materials* **184** (1–3), 746–752.

Babatunde, A., Zhao, Y., Burke, A. M., Morris, M. A. & Hanrahan, J. P. 2009 Characterization of aluminium-based water treatment residual for potential phosphorus removal in engineered wetlands. *Environmental Pollution* **10** (157), 2830–2836.

Barca, C., Troesch, S., Meyer, D., Drissen, P., Andres, Y. & Chazarenc, F. 2013 Steel slag filters to upgrade phosphorus removal in constructed wetlands: two years of field experiments. *Environmental Science & Technology* **47** (1), 549–556.

Chen, J., Cai, Y., Clark, M. & Yu, Y. 2013 Equilibrium and kinetic studies of phosphate removal from solution onto a hydrothermally modified oyster shell material. *PLoS One* **8** (4), e60243.

Clark, M. W., Akhurst, D. J. & Fergusson, L. 2012 Removal of radium from groundwater using a modified bauxite refinery residue. *Journal of Environment Quality* **41** (1), 296.

Fu, J., Chen, Y. J., Ju, J. Y., Li, Q. S., An, S. Q. & Zhu, H. L. 2010 Treating dye wastewater of reactive brilliant red K-2BP by cetyltrimethylammonium chloride-modified bentonite with polyacrylamide flocculant. *Polish Journal of Environmental Studies* **20** (1), 61–66.

Han, R., Li, Y., Zhang, J., Zhang, L., Xie, F., Cheng, J. & Zhao, Z. 2008 Langmuir isotherm and pseudo second order kinetic model for the biosorption of methylene blue onto rice husk. In: *IEEE*, pp. 3545–3548.

Jie Fu, R. S. W. M. & Zhua, A. H. 2010 Adsorption of disperse blue 2BLN by microwave activated red mud. *Environmental Progress & Sustainable Energy* **30** (4), 558–566.

Liu, W., Zhao, X., Wang, T., Fu, J. & Ni, J. 2015 Selective and irreversible adsorption of mercury from aqueous solution by a flower-like titanate nanomaterial. *Journal of Materials Chemistry A* **3** (34), 17676–17684.

Qin, J., Cui, X., Cui, C., Hussain, A. & Yang, C. 2015 Preparation and characterization of ceramsite from lime mud and coal fly ash. *Construction and Building Materials* **95** (1), 10–17.

Tercero, M. D. C., Álvarez-Rogel, J., Conesa, H. M., Párraga-Aguado, I. & González-Alcaraz, M. N. 2017 Phosphorus retention and fractionation in an eutrophic wetland: a one-year mesocosms experiment under fluctuating flooding conditions. *Journal of Environmental Management* **190** (1), 197–207.

Vohla, C., Kõiv, M., Bavor, H. J., Chazarenc, F. & Mander, Ü. 2011 Filter materials for phosphorus removal from wastewater in treatment wetlands – a review. *Ecological Engineering* **37** (1), 70–89.

Wei, X., Viadero, R. C. & Bhojappa, S. 2008 Phosphorus removal by acid mine drainage sludge from secondary effluents of municipal wastewater treatment plants. *Water Research* **42** (13), 3275–3284.

Xu, G. R., Zou, J. L. & Li, G. B. 2009 Ceramsite obtained from water and wastewater sludge and its characteristics affected by $(Fe_2O_3 + CaO + MgO)/(SiO_2 + Al_2O_3)$. *Water Research* **43** (11), 2885–2893.

Yang, L., Chang, H. & Huang, M. L. 2001 Nutrient removal in gravel- and soil-based wetland microcosms with and without vegetation. *Ecological Engineering* **18** (1), 91–105.

Yang, Y., Zhao, Y., Babatunde, A., Wang, L., Ren, Y. & Han, Y. 2006 Characteristics and mechanisms of phosphate adsorption on dewatered alum sludge. *Separation and Purification Technology* **2** (51), 193–200.

Yin, H., Yan, X. & Gu, X. 2017 Evaluation of thermally-modified calcium-rich attapulgite as a low-cost substrate for rapid phosphorus removal in constructed wetlands. *Water Research* **115** (15), 329–338.

Zhao, Y. Q. 2006 Involvement of gypsum ($CaSO_4{\cdot}2H2O$) in water treatment sludge dewatering: a potential benefit in disposal and reuse. *Separation Science and Technology* **12** (41), 2785–2794.

First received 10 April 2019; accepted in revised form 23 July 2019. Available online 30 July 2019